Study of Cluster Structure of Light Nuclei by Feynman's Continual Integrals and Hyperspherical Functions

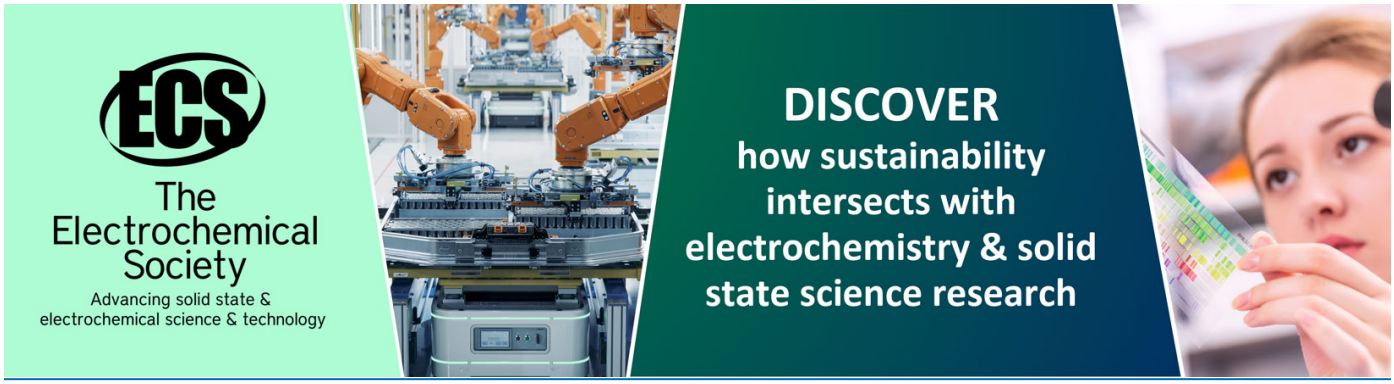

Study of Cluster Structure of Light Nuclei by Feynman's Continual Integrals and Hyperspherical Functions

V V Samarin[1,2]

[1]Joint Institute for Nuclear Research, 6 Joliot-Curie Street, Dubna, Moscow Region, 141980, Russia
[2]Dubna State University, 19 Universitetskaya Street, Dubna, Moscow Region, 141982, Russia

samarin@jinr.ru

Abstract. Calculations of the probability densities and energies for *N*α-cluster nuclei ^{12}C (3α), ^{16}O (4α), ^{20}Ne (5α), ^{24}Mg (6α), ^{28}Si (7α) and for nuclear molecules ^{9}Be (α + *n* + α), ^{10}Be (α + *n* + *n* + α), were performed by the Feynman's continual integrals method using parallel computing based on NVIDIA CUDA technology. New effective method for the solution of the hyperradial equations with cubic splines approximation is proposed and tested for exactly solvable 4-body system.

1. Feynman's continual integrals method for nuclear molecules and *N*α-cluster nuclei

Feynman's continual integral (FCI) [1] is a propagator $K(\vec{q},t;\vec{q}_0,0)$ — the probability amplitude for a particle to travel in the *s*-dimensional space from one point ($\vec{q}_0$) to another ($\vec{q}$) in a given time *t*. For a time-independent potential energy $V(\vec{q})$, transition to the imaginary time $t = -i\tau$ yields the propagator $K_{\mathrm{E}}(\vec{q},t;\vec{q}_0,0)$ with the asymptotic behavior [2]

$$K_{\mathrm{E}}(\vec{q},\tau;\vec{q},0) \to |\psi_0(\vec{q})|^2 \exp\left(-\frac{E_0\tau}{\hbar}\right) + |\psi_1(\vec{q})|^2 \exp\left(-\frac{E_1\tau}{\hbar}\right) + \ldots, \ \tau \to \infty, \qquad (1)$$

here E_0, E_1 are the energies of ground and first excited states with the wave functions $\psi_0(\vec{q})$, $\psi_1(\vec{q})$. The values of the propagator $K_{\mathrm{E}}(\vec{q},\tau;\vec{q}_0,0)$ were calculated using averaging over random trajectories with the distribution in the form of the multidimensional Gaussian distribution [3]. Parallel calculations [4] by the Monte Carlo method using NVIDIA CUDA technology [5, 6] were performed on the Heterogeneous Cluster [7] of the Joint Institute for Nuclear Research. For nuclear systems the dimensionless variables are used

$$\tilde{K}_{\mathrm{E}}\left(\vec{\tilde{q}},\tilde{\tau};\vec{\tilde{q}},0\right) \approx \left(\frac{\tilde{m}}{2\pi\tilde{\tau}}\right)^{s/2} \left\langle \exp\left[-\Delta\tilde{\tau} b_0 \sum_{k=1}^{N} \tilde{V}(\vec{\tilde{q}}_k)\right]\right\rangle_{0,N}, \qquad (2)$$

here $\tilde{K}_{\mathrm{E}} = K_{\mathrm{E}} x_0^s$, $\vec{\tilde{q}} = \vec{q}/x_0$ $x_0 = 1$ fm, $\tilde{m} = m/m_0$, m_0 is the neutron mass, $\tilde{V} = V/\varepsilon_0$, $\varepsilon_0 = 1$ MeV, $\tilde{\tau} = \tau/t_0$, $\Delta\tilde{\tau} = \Delta\tau/t_0$, $t_0 = m_0 x_0^2/\hbar \approx 1.57\cdot 10^{-23}$ s, $b_0 = t_0\varepsilon_0/\hbar \approx 0.02412$. The equation

$$b_0^{-1}\ln\tilde{K}_{\mathrm{E}}\left(\vec{\tilde{q}},\tilde{\tau};\vec{\tilde{q}},0\right)\approx b_0^{-1}\ln\left|\psi_0(\vec{\tilde{q}})\right|^2-\tilde{E}_0\tilde{\tau} \tag{3}$$

can be used to obtain the dimensionless energy $\tilde{E}_0 = E_0/\varepsilon_0$ as the slope of the linear part of the graph representing $\ln\tilde{K}_{\mathrm{E}}$ as a function of $\tilde{\tau}$.

1.1. The verification testing of the FCI method for exactly solvable 5-body system

The verification testing of the FCI method for exactly solvable *N*-body systems for *N* =2, 3, 4 was made in [3, 8]. For a exactly solvable 5-body system the FCI calculations are demonstrated on the example of the simple model. Light particles 1, 2, 3, 4 with masses $m_i = m_0$, $i = 1,\ldots 4$ interact only with infinitely heavy particle 5 with $m_5 = \infty$ by potential $V(r)$ with the repulsive core (see figure 1a)

$$V(r) = \sum_{k=1}^{3} u_k \exp\left(-r^2/b_k^2\right). \tag{4}$$

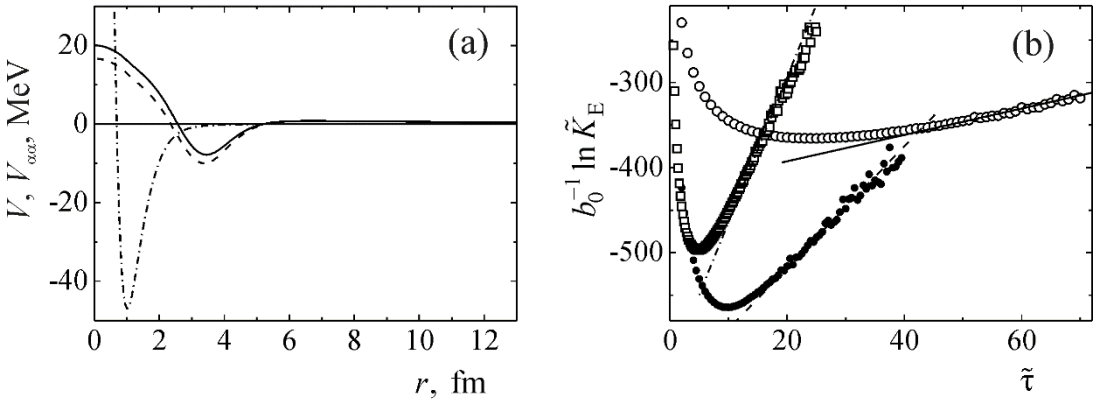

Figure 1. (a) The potential $V(r)$ (3) of interaction of infinitely heavy particle with independent particles in the model 5-body system (dash-dotted curve) and α–α potentials $V_{\alpha\alpha}(r)$ with nuclear part (5) for ^{9}Be (solid curve) and ^{10}Be (dashed curve). (b) The logarithm $\ln\tilde{K}_{\mathrm{E}}$ of the dimensionless propagator as a function of dimensionless variable $\tilde{\tau}$ for model 5-body system (squares) , ^{9}Be (circles) and ^{10}Be(points); the dash-dotted, solid and dashed lines are the results of the linear regression.

The radial Schrödinger equation was solved numerically by difference scheme for 2-body system of particles 1 and 5. The ground state energy is equal to –4 MeV for parameters values: $u_1 = 500$ MeV, $u_2 = -102$ MeV, $u_3 = -2$ MeV, $b_1 = 0.50$ fm, $b_2 = 1.265$ fm, $b_3 = 2.67$ fm [8]. The ground state energy of the model 5-body system is equal to the sum of ground state energies of particles 1, 2, 3, 4, i.e. $E_0 = -16$ MeV. The calculation using Jacobian coordinates with statistics $3\cdot10^7$ random trajectories and $\tilde{\tau} = 0.001$ yields (see figure 1b) the result of linear regression of dependence (3) $E_0 = -16.15 \pm 0.60$ MeV, i.e., the absolute and relative errors are small.

1.2. The nuclear molecules ^{9}Be (α + n + α) and ^{10}Be (α + n + n + α)

The repulsive core is the typical property of nucleon-nucleon potentials $V_{NN}(r)$, e.g. M3Y potential [9], and of the α–α potentials $V_{\alpha\alpha}(r)$ of interaction of α–particles (α–clusters) [10, 11]. For

description of *Nα*-nuclei (^{12}C, ^{16}O etc.) and nuclear "molecules" ^{9}Be ($\alpha + n + \alpha$), ^{10}Be ($\alpha + n + n + \alpha$) [12–15] nuclear part of the α–α potential $V_{\alpha\alpha}^{(N)}(r)$ is used in the form

$$V_{\alpha\alpha}^{(N)}(r) = -U_{\alpha 1} f(r; B_{\alpha 1}, a_{\alpha 1}) + U_{\alpha 2} f(r; B_{\alpha 2}, a_{\alpha 2}), \quad (5)$$

here $f(r; B, a)$ is the function of Woods-Saxon type

$$f(r; B, a) = \left[1 + \exp\left(\frac{r - B}{a}\right)\right]^{-1}. \quad (6)$$

Total α–α potential includes nuclear and Coulomb parts $V_{\alpha\alpha}(r) = V_{\alpha\alpha}^{(N)}(r) + V_{\alpha\alpha}^{(C)}(r)$, typical plots of $V_{\alpha\alpha}(r)$ are shown in the figure 1a. The potentials $V_{\alpha n}(r)$ of interaction of α–particles (α–clusters) with neutron and $V_{nn}(r)$ of interaction of neutrons were determined in [3, 16] based on FCI calculation of ground state energy for nuclei ^{3}H, ^{6}He, ^{6}Li, ^{7}Li.

Experimental values of energy of separation to α–clusters and neutrons are equals to 1.57 MeV for ^{9}Be nucleus and 8.38 МэВ for ^{10}Be nucleus [17]. The results of the calculation of the propagator $K_{\mathrm{E}}(\vec{q}, t; \vec{q}_0, 0)$ using Jacobian coordinates for nuclei nuclear "molecules" ^{9}Be and ^{10}Be with statistics $15 \cdot 10^6$ random trajectories and $\tilde{\tau} = 0.01$ are shown in figure 1b. The results of linear regression of dependence (3) are $E_0 = -1.57 \pm 0.3$ MeV for ^{9}Be nucleus and $E_0 = -8.3 \pm 0.7$ MeV for ^{10}Be nucleus., i.e., the absolute and relative differences from experimental values are small. Values of parameters of potential (4) are: $B_{\alpha 1}$ = 3.73 fm, $B_{\alpha 2}$ = 2.71 fm, $a_{\alpha 1} = a_{\alpha 2} = 0.512$ fm, $U_{\alpha 2} = 38$ MeV for both nuclei, $U_{\alpha 1}$ = 27.44 MeV for ^{9}Be nucleus and $U_{\alpha 1} = 33$ MeV for ^{10}Be nucleus. Small difference in values of the parameter $U_{\alpha 1}$ and in the potential $V_{\alpha\alpha}(r)$ for the ^{9}Be and ^{10}Be nuclei may be explained by different polarizations of α–clusters in these nuclei. The probability density for ground state of ^{9}Be is shown in [8, 18]. For ^{10}Be nucleus the probability densities for some configurations of ground state with Jacobian vectors $\vec{y} \perp \vec{x}, \vec{y} \perp \vec{z}$ are shown in figure 2

$$\vec{x} = \vec{r}_{\alpha_2} - \vec{r}_{\alpha_1}, \ \vec{y} = \vec{r}_{n_2} - \vec{r}_{n_1}, \ \vec{z} = \frac{1}{2}\left(\vec{r}_{n_1} + \vec{r}_{n_2}\right) - \frac{1}{2}\left(\vec{r}_{\alpha_2} + \vec{r}_{\alpha_1}\right). \quad (7)$$

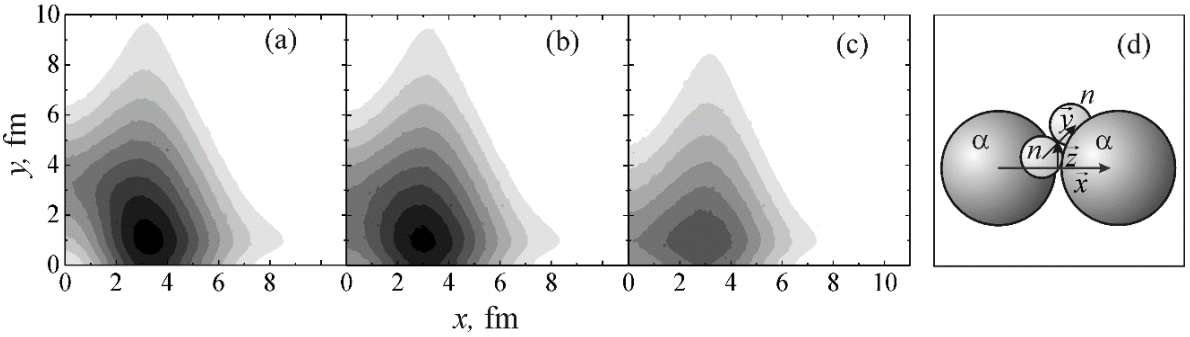

Figure 2. (a–c) The probability densities for some configurations of the ground state of ^{10}Be nucleus with Jacobian vectors $\vec{y} \perp \vec{x}, \vec{y} \perp \vec{z}$ for $z = 0$ (a), $z = 1$ fm (b), $z = 2.5$ fm (c); the logarithmic tone scale is used. (d) Jacobian vectors and 3D model of system ($\alpha + n + n + \alpha$).

The most probable configuration has neutron "cloud" between α–clusters (see figures 2a,b). Near the inter α–clusters axis this "cloud" consists from di-neutron cluster mainly (black areas in figures 2a,b).

1.3. The Nα-cluster nuclei ^{16}O, ^{20}Ne, ^{24}Mg, ^{28}Si

Experimental values of energy of separation of *N*α-cluster nuclei ^{16}O, ^{20}Ne, ^{24}Mg, ^{28}Si to α–clusters are listed in the table 1 [17].

Table 1. Experimental and calculated values of the energy of the separation to α–clusters for *N*α-cluster nuclei.

*N*α-cluster nuclei	Experimental values (MeV) [17]	Calculated values (MeV)
^{12}C (3α)	−7.27	−6.82±0.4
^{16}O (4α)	−14.44	−13.7±0.6
^{20}Ne (5α)	−19.165	−23.1±0.8
^{24}Mg (6α)	−28.481	−30.2±1.0
^{28}Si(7α)	−38.465	−47.5±1.5

The universal α–α potentials $V_{\alpha\alpha}(r)$ with nuclear part (5) similar to potential for ^{10}Be was used in the calculations (see figure 3a). Values of parameters of potential (5) are: $B_{\alpha 1}$ = 3.73 fm, $B_{\alpha 2}$ = 2.71 fm, $a_{\alpha 1} = a_{\alpha 2} = 0.512$ fm, $U_{\alpha 1}$ = 29 MeV, $U_{\alpha 2} = 38$ MeV. The results of the calculation of the propagator $K_{\mathrm{E}}(\vec{q},t;\vec{q}_0,0)$ using Jacobian coordinates are shown in figure 3b. The results of linear regression of dependence (3) yields the result listed in the table 1. The calculations with universal α-α-potential reproduce experimental values of separation energy approximately. The individual small variations of potential may be included for accurate coincidence with experimental values. More correct α-α potential must become weaker for transfer from ^{20}Ne to ^{28}Si nuclei.

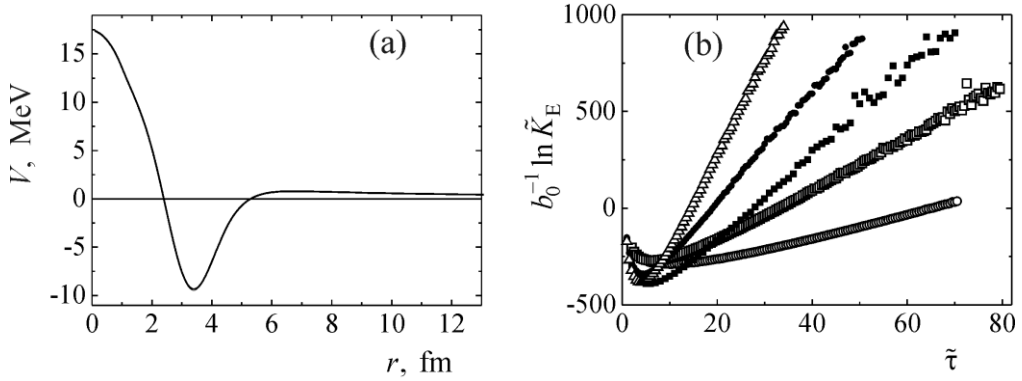

Figure 3. (a) The universal α–α potentials $V_{\alpha\alpha}(r)$ with nuclear part (5) for *N*α-cluster nuclei ^{12}C, ^{16}O, ^{20}Ne, ^{24}Mg, ^{28}Si. (b) The logarithm $\ln\tilde{K}_{\mathrm{E}}$ of the dimensionless propagator as a function of dimensionless variable $\tilde{\tau}$ for *N*α-cluster nuclei ^{12}C (circles), ^{16}O (empty squares), ^{20}Ne (squares), ^{24}Mg (points), ^{28}Si (triangles).

The ground state of ^{12}C nucleus regarded as system of three α–clusters was studied in [19]. For the ground state, the most probable configuration is a regular triangle of α-clusters. The probability density distribution for ^{24}Mg (6α) nucleus is shown in figure 4. Probability density is consistent with

potential landscape and it validates the correctness of the calculations. Most probable configuration is a pair of the regular triangle of α-clusters. Two-triangles configuration may be represented as combination of two carbon clusters $^{12}C(3\alpha) + {}^{12}C(3\alpha)$.

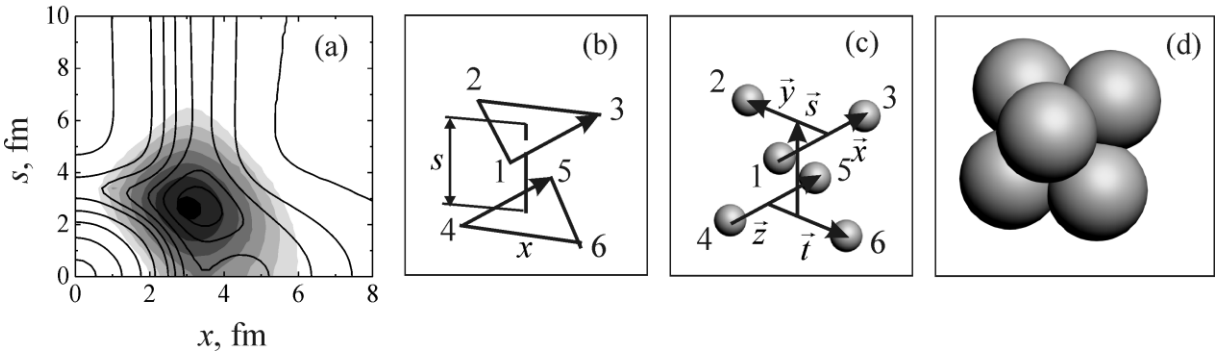

Figure 4. (a) The probability densities (shade of grey in logarithmic scaling) for two-triangles configuration of the ground state of $^{24}Mg(6\alpha)$ nucleus with potential landscape (curves). (b) The dimensions of the two-triangles configuration. (c) The five Jacobian vectors in the case of $\vec{x} \perp \vec{y}$, $\vec{y} \perp \vec{s}$, $\vec{x} \parallel \vec{z}$, $\vec{y} \parallel \vec{t}$. (d) 3D model of system $^{24}Mg(6\alpha)$.

For $^{16}O(4\alpha)$ nucleus a tetrahedron configuration with edge 3.4 ± 0.4 fm is the most probable, it is evident result. The most probable configuration for $^{20}Ne(5\alpha)$ is like to two conjunct tetrahedrons (see figure 5).

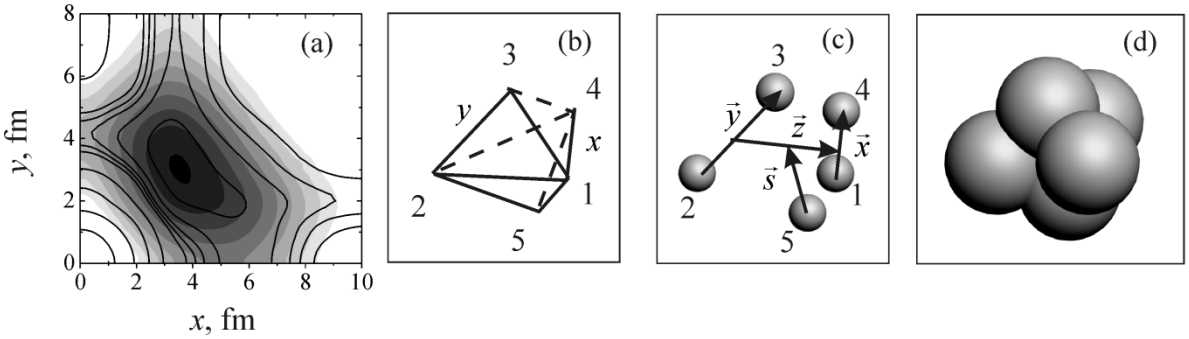

Figure 5. (a) The probability densities (shade of grey in logarithmic scaling) for two-tetrahedron configuration of the ground state of $^{20}Ne(5\alpha)$ nucleus with potential landscape (curves). (b) The dimensions of the two-tetrahedrons configuration. (c) The four Jacobian vectors $\vec{x}$, $\vec{y}$, $\vec{z}$, $\vec{s}$. (d) 3D model of system $^{20}Ne(5\alpha)$.

The two more probable configurations of ground state of $^{28}Si(7\alpha)$ nucleus are shown in figure 6.

2. Spline approximation for solving hyperradial equations

The Schrödinger equation was solved by expansion of wave functions into hyperspherical functions (HSF) [20] for few three-body systems, *e.g.*, for ^{9}Be [21], ^{6}He and ^{12}C [22]. The main problem of this approach is the numerical solution of the so-called hyperradial equations. For the states with zero total angular momentum $L = 0$ the hyperradial equations for three-body systems are

$$\frac{d^2}{d\rho^2}\varphi_{K0}^{l_x l_x}(\rho) + \left[\frac{2}{\hbar^2}\varepsilon - \frac{(K+3/2)(K+5/2)}{\rho^2}\right]\varphi_{K0}^{l_x l_x}(\rho) = \frac{2}{\hbar^2}\sum_{K'l'_x} U_{KK'00}^{l_x l_x; l'_x l'_x}(\rho)\varphi_{K'0}^{l'_x l'_x}(\rho) \qquad (8)$$

with the coupling matrix

$$U^{l_x l_x;l'_x l'_x}_{KK'00}(\rho) = \langle l_x l_x K0 | U | l'_x l'_x K'0 \rangle . \tag{9}$$

Here ε and U are the total and potential energies of the system, ρ is the hyperradius, K is the hypermomentum, l_x is the angular momentum of a pair of particles of the system.

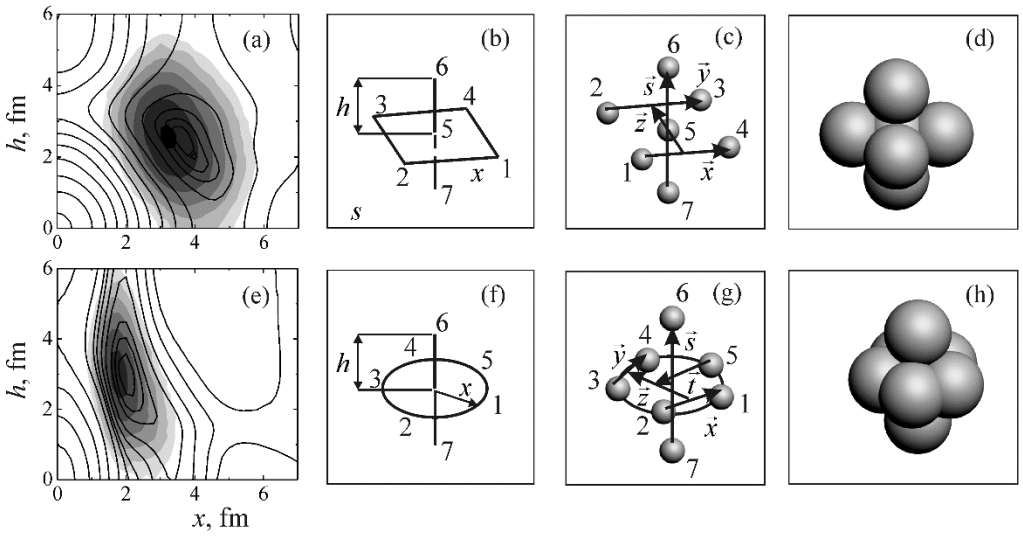

Figure 6. (a, e) The probability densities (shade of grey in logarithmic scaling) for the ground state of ^{28}Si(7α) nucleus with potential landscape (curves). (b, f) The dimensions of the two configurations. (c, g) The four (c) and five (g) vectors from six Jacobian vectors. (d, h) 3D models of system ^{28}Si(7α).

The analogous hyperradial equations for four-body systems with zero total angular momentum L are

$$\frac{d^2}{d\rho^2}\chi^{l_x l_y l_{xy} l_z}_{\mu KL}(\rho) - \left[\frac{2}{\hbar^2}\varepsilon + \frac{(\mu+3)(\mu+4)}{\rho^2}\right]\chi^{l_x l_y l_{xy} l_z}_{\mu KL}(\rho) = \sum_{\mu' K' l'_x l'_y l'_{xy} l'_z} W^{l_x l_y l_{xy} l_z;l'_x l'_y l'_{xy} l'_z}_{\mu K \mu' K'}(\rho)\chi^{l'_x l'_y l'_{xy} l'_z}_{\mu' K' L}(\rho) \tag{10}$$

μ is the hypermomentum. There are several laborious methods of solving hyperradial equations, *e.g.*, using the basis of the Lagrange functions [21, 22]. New method of solving hyperradial equations using cubic spline approximation [23] was proposed in [8]. The idea of this method is the simultaneous calculation of the mesh function $\varphi^{l_x l_x}_{KL,i} = \varphi^{l_x l_x}_{KL}(\rho_i)$ and its second derivative $m^{l_x l_x}_{KL,i} = d^2\varphi^{l_x l_x}_{KL}(\rho)/d\rho^2\big|_{\rho_i}$.

The difference equations on the mesh for differential equations (8) are

$$-\boldsymbol{A}^{-1}\boldsymbol{H}\boldsymbol{\varphi}^{l_x l_x}_{K0} + \frac{1}{\rho_i^2}(K+3/2)(K+5/2)\varphi^{l_x l_x}_{K0,i} + \sum_{K',l'_x}\varphi^{l'_x l'_x}_{K'0,i}\frac{2}{\hbar^2}U^{l_x l_x;l'_x l'_x}_{KK'00}(\rho_i) = \frac{2}{\hbar^2}\varepsilon\varphi^{l_x l_x}_{K0,i} \tag{11}$$

The matrices $\boldsymbol{A}$ and $\boldsymbol{H}$ were defined in [23]. System (11) is the eigenvalue problem $\boldsymbol{B\Phi} = \lambda\boldsymbol{\Phi}$, where energies are eigenvalues of matrix $\boldsymbol{B}$, and wave functions are eigenvectors of matrix $\boldsymbol{B}$. This modified method has some advantages. The main advantage is the smooth interpolation between mesh points with natural boundary conditions $m^{l_x l_x}_{K0,0} = m^{l_x l_x}_{K0,N} = 0$. Another advantage is a small size of the matrix for a special choice of the non-uniform mesh and fast calculations, but only for the ground state. This method was tested for the exactly solvable harmonic oscillator and nuclear 3-body systems in [8]. The convergence to the exact solution is fast for the pairwise parabolic interaction potential (at $K > 4$) and

slow for the pairwise interaction with a repulsive core (at $K > 40$). For the exactly solvable 4-body harmonic system with equal masses m and the pairwise parabolic potentials

$$V_{ij}(r_{ij}) = \frac{m\omega^2}{2} r_{ij}^2,\ V = \sum_{i<j} V_{ij}(r_{ij}) = \frac{m\omega^2}{2}\left(r_{12}^2 + r_{13}^2 + r_{14}^2 + r_{23}^2 + r_{24}^2 + r_{34}^2\right) . \quad (12)$$

the convergence is fast. Exact values of energy for $m=1,\ \omega=1,\ \hbar=1$ are $E_n = 4n + 2l + 3 = 9,\ 13,\ldots;\ l = 3$. For exact value $E_0 = 9$ calculated value with step $\Delta\rho = 0.5$ is $E_0 = 9.13$ and for exact value $E_1 = 13$ calculated value is E_1=13.6.

Acknowledgments

Author wishing to acknowledge HybriLIT team by technical support of parallel calculations on the Heterogeneous Cluster of the Joint Institute for Nuclear Research.

References

[1] Feynman R P and Hibbs A R 1965 *Quantum Mechanics and Path Integrals* (New York: McGraw-Hill)
[2] Shuryak E V and Zhirov O V 1984 *Nucl. Phys.* B **242** 393
[3] Samarin V V and Naumenko M A 2017 *Phys. Atom. Nucl*. **80** 877
[4] Samarin V V and Naumenko M A 2016 *Supercomp. Front. Innov*. **3** 80
[5] NVIDIA CUDA, http://developer.nvidia.com/cuda-zone/
[6] Sanders J and Kandrot E 2011 *CUDA by Example: An Introduction to General-Purpose GPU Programming* (New York: Addison-Wesley)
[7] Heterogeneous Cluster, Joint Institute for Nuclear Research, http://hybrilit.jinr.ru/
[8] Samarin V V 2017 *Proc. Int. Workshop on Nuclear Theory (Rila Mountains, Bulgaria)* vol 36 (Sofia: Heron Press) p 233
[9] Satchler G R and Love W G 1979 *Phys. Rep.* **55** 183
[10] Bando H 1986 *Nucl. Phys.* A **450** 217
[11] Michel F, Ohkubo S and Reidemeister G 1998 Prog. *Theor. Phys. Suppl*. **132** 132
[12] von Oertzen W 1996 *Z. Phys. A* **354** 37
[13] von Oertzen W, Freer M and Kanada-En'yo Y 2006 *Phys. Rep.* **432** 43
[14] Okabe S, Abe Y and Tanaka H 1977 *Prog. Theor. Phys.* **57** 866
[15] Okabe S and Abe Y. 1979 *Prog. Theor. Phys*. **61** 1049
[16] Samarin V V and Naumenko M A 2019 *Bull. Russ. Acad. Sci.: Phys.* **83** 411
[17] Zagrebaev V I, Denikin A S, Karpov A V et al. *NRV web knowledge base on low-energy nuclear physics*. http://nrv.jinr.ru/
[18] Samarin V V 2019 *Book of Abstr. Int. Conf. NUCLEUS-2019 (Dubna, Russia)* (Dubna: JINR) p 240 https://indico.jinr.ru/event/706/material/12/0
[19] Samarin V V and Naumenko M A 2019 *Il Nuovo Cimento* **42 C** 130
[20] Dzhibuti R I and Shitikova K V 1993 *Method of Hyperspherical Functions in Atomic and Nuclear Physics* (Moscow: Energoatomizdat) in Russian
[21] Descouvemont P, Druet T, Canto L F and Hussein M S 2015 *Phys. Rev. C* **91** 024606
[22] Descouvemont P, Daniel C and Baye D 2003 *Phys. Rev. C* **67** 044309
[23] Marchuk G I 1982 *Methods of Numerical Mathematics* (New York: Springer-Verlag)